Published in "Molecular Microbiology doi: 10.1111/mmi.13427, 2016"
which should be cited to refer to this work.

RflM mediates target specificity of the RcsCDB phosphorelay system for transcriptional repression of flagellar synthesis in *Salmonella enterica*

Caroline Kühne,[1] Hanna M. Singer,[2,3] Eva Grabisch,[1] Luca Codutti,[4] Teresa Carlomagno,[4,5] Andrea Scrima[6] and Marc Erhardt[1]*

[1]*Junior Research Group Infection Biology of Salmonella, Helmholtz Centre for Infection Research, 38124 Braunschweig, Germany.*
[2]*Microbiologie, Département de Médecine, Université de Fribourg, 1700 Fribourg, Switzerland.*
[3]*Helmholtz Centre for Infection Research, 38124 Braunschweig, Germany.*
[4]*Centre of Biomolecular Drug Research (BMWZ), Leibniz University Hannover, 30167 Hannover, Germany.*
[5]*Group of Structural Chemistry, Helmholtz Centre for Infection Research, 38124 Braunschweig, Germany.*
[6]*Junior Research Group Structural Biology of Autophagy, Helmholtz Centre for Infection Research, 38124 Braunschweig, Germany.*

Summary

The bacterial flagellum enables directed movement of *Salmonella enterica* towards favorable conditions in liquid environments. Regulation of flagellar synthesis is tightly controlled by various environmental signals at transcriptional and post-transcriptional levels. The flagellar master regulator $FlhD_4C_2$ resides on top of the flagellar transcriptional hierarchy and is under autogenous control by $FlhD_4C_2$-dependent activation of the repressor *rflM*. The inhibitory activity of RflM depends on the presence of RcsB, the response regulator of the RcsCDB phosphorelay system. In this study, we elucidated the molecular mechanism of RflM-dependent repression of *flhDC*. We show that RcsB and RflM form a heterodimer that coordinately represses *flhDC* transcription independent of RcsB phosphorylation. RcsB-RflM complex binds to a RcsB box downstream the P1 transcriptional start site of the *flhDC* promoter with increased affinity compared to RcsB in the absence of RflM. We propose that RflM stabilizes binding of unphosphorylated RcsB to the *flhDC* promoter in absence of environmental cues. Thus, RflM is a novel auxiliary regulatory protein that mediates target specificity of RcsB for *flhDC* repression. The cooperative action of the RcsB-RflM repressor complex allows *Salmonella* to fine-tune initiation of flagellar gene expression and adds another level to the complex regulation of flagellar synthesis.

*For correspondence. E-mail marc. erhardt@helmholtz-hzi.de; Tel. +49-531-6181-4801; Fax +49-531- 6181-5709.

Introduction

The Gram-negative enterobacterium *Salmonella enterica* serovar Typhimurium is a causative agent of the foodborne illness Salmonellosis resulting in self-limiting gastroenteritis and in rare cases in systemic bacteremia that can be life-threatening (Hohmann, 2001). *Salmonella* uses several virulence factors to establish successful infection of host cells including the secretion of effector molecules through needle-like secretion systems (injectisomes) encoded on *Salmonella* pathogenicity islands (Spi) and flagellar-mediated motility. Flagella are rotary motility organelles that enable directed movement in liquid environment, attachment to host cells and promotion of biofilm formation (Duan *et al.*, 2013).

The bacterial flagellum is a complex nanomachine made of dozens of different proteins that need to self-assemble in an ordered, regulated process for the formation of a functional motility organelle. The flagellar regulon comprises more than 60 genes involved in synthesis of the flagellum of *Salmonella* and is controlled at various levels (Frye *et al.*, 2006). The synthesis and assembly of the bacterial flagellum is hierarchically organized and tightly regulated at the level of gene expression. At top of the flagellar synthesis cascade resides the flagellar master operon *flhDC* that is transcribed from a flagellar class 1 promoter producing the heteromultimeric $FlhD_4C_2$

complex. This complex activates σ^{70}-dependent transcription of genes from flagellar class 2 promoters that encode the hook-basal-body (HBB) structure, the alternative sigma factor σ^{28} (FliA) and the anti-sigma factor FlgM. Upon HBB completion, the anti-sigma factor is secreted, releasing σ^{28} and allowing for σ^{28}-dependent transcription from flagellar class 3 promoters, whose gene products encode the filament and rotary motor components (Chilcott and Hughes, 2000; Karlinsey *et al.*, 2000; Chevance and Hughes, 2008).

The flagellar master regulator $FlhD_4C_2$ is the major checkpoint for initiation of flagellar synthesis and is under extensive control by various environmental and regulatory signals. Several global regulators activate transcription of the *flhDC* operon, including the cyclic AMP-catabolite repressor protein (cAMP-CRP), the histone-like nucleoid-structuring protein (H-NS) and the nucleoid-organization protein Fis (Kutsukake, 1997; Kelly *et al.*, 2004). The main regulator of the Spi-1 injectisome system, HilD, binds upstream of the *flhDC* P5 transcriptional start site and thereby activates *flhDC* transcription (Singer *et al.*, 2014). Posttranscriptional activation of *flhDC* occurs at the level of the flagellar regulator FliZ via regulation of HilD activity and repression of the anti-$FlhD_4C_2$ factor YdiV (Chubiz *et al.*, 2010; Wada *et al.*, 2011). YdiV is a posttranscriptional repressor of $FlhD_4C_2$ responsible for nutritional control by targeting $FlhD_4C_2$ complex to ClpXP-dependent degradation (Takaya *et al.*, 2012; Koirala *et al.*, 2014). Another anti-$FlhD_4C_2$ factor is the flagellar-related protein FliT, which interacts with free FlhC subunits preventing activation of flagellar class 2 promoter transcription and leading to ClpXP-dependent proteolysis (Yamamoto and Kutsukake, 2006; Aldridge *et al.*, 2010; Sato *et al.*, 2014).

Multiple other DNA-binding proteins act upon the *flhDC* promoter to repress transcription of the *flhDC* operon. These include the Spi-1 encoded repressor RtsB, as well as LrhA, SlyA and RcsB (Lehnen *et al.*, 2002; Ellermeier and Slauch, 2003; Wang *et al.*, 2007; Erhardt and Hughes, 2010). The RcsB protein is the response regulator of the RcsCDB phosphorelay system that is involved in many regulatory processes. The phosphorelay is initiated by autophosphorylation of the sensor kinase RcsC followed by transfer of the phosphoryl group via the intermediate molecule RcsD to the response regulator RcsB. Phosphorylated RcsB is able to regulate target genes by DNA-binding as a homodimer or after heterodimerization with auxiliary proteins (Majdalani and Gottesman, 2005; Huang *et al.*, 2006). Activation of the RcsCDB phosphorelay in *S. enterica* is stimulated by environmental changes concerning osmolarity, oxidative stress and affecting the bacterial envelope integrity (Huang *et al.*, 2006). The outer membrane lipoprotein RcsF senses envelope stress induced by cationic antimicrobial peptides and activates autophosphorylation of RcsC (Farris *et al.*, 2010). In contrast, the intracellular growth attenuator IgaA represses the Rcs system by preventing RcsB phosphorylation via the RcsCDB phosphorelay (Mariscotti and García-del Portillo, 2009). Conditions with low or high osmolarity result in activation of the Rcs system leading to repression or activation of target genes, respectively, (Arricau *et al.*, 1998).

In *S. enterica*, the RcsCDB regulon comprises a variety of target genes that are regulated by RcsB alone or together with the auxiliary protein RcsA. RcsA is an unstable protein, but an interaction between RcsA and RcsB stabilizes RcsA, allowing RcsAB to bind to a RcsAB box of target DNA (Stout *et al.*, 1991; Wehland and Bernhard, 2000). Initially, RcsB was identified as a positive regulator in *Escherichia coli* colonic acid capsule synthesis (Sledjeski and Gottesman, 1996). In *S. enterica*, RcsB together with RcsA activates transcription of envelope biosynthetic genes. The *ugd* gene encoding UDP-glucose dehydrogenase, which enables colonic acid and lipopolysaccharide (LPS) 4-aminoarabinose production, and the capsule synthesis operon *cps* are positively regulated under RcsB activating conditions (Mouslim *et al.*, 2003). Gene targets regulated by RcsB independently from RcsA are involved in motility, virulence, survival and other physiological processes. RcsB activates transcription of genes involved in physiological processes like the wzz_{st} gene responsible for correct LPS O-antigen formation and the *dps* gene involved in oxidative stress resistance (Delgado *et al.*, 2006; Farizano *et al.*, 2014). The biofilm master regulatory gene *csgD* is activated by unphosphorylated RcsB, but repressed upon RcsB phosphorylation (Latasa *et al.*, 2012). RcsB is required for activation of genes encoding the Spi-2 injectisome. Thus, the Rcs system is important for Spi-2 dependent late stages of *Salmonella* infection in mice (Detweiler *et al.*, 2003; Wang *et al.*, 2007). In contrast, activated RcsB inhibits transcription of genes belonging to the Spi-1 regulon, as well as the Spi-2 effector molecule *srfJ* and constitutive activation of the Rcs system results in attenuation of virulence (Mouslim *et al.*, 2004; García-Calderón *et al.*, 2005, 2007; Lin *et al.*, 2008; Cordero-Alba *et al.*, 2012). RcsB displays a dual regulatory function concerning motility. In *E. coli* flagellar motility is negatively regulated by RcsB and RcsA binding to the RcsAB box of the promoter of the flagellar master regulator *flhDC* (Francez-Charlot *et al.*, 2003). In contrast, RcsA is not required for *flhDC* repression in *S. enterica* (Wang *et al.*, 2007). Flagellar motility is increased by RcsB-dependent antisense transcription of the *fliPQR* genes encoding for integral membrane components of the flagellar export apparatus. The antisense *fliPQR* transcript thereby controls the correct stoichiometry of the FliPQR proteins (Wang *et al.*, 2007; Wang and Harshey, 2009).

RflM, a negative regulator of the flagellar master operon *flhDC* was identified in a transposon screen for new flagellar regulators in *Salmonella* (Wozniak *et al*., 2009). RflM functions by repression of *flhDC* transcription. Transcription of *rflM* is dependent on $FlhD_4C_2$ and both RflM and the Rcs system participate in an auto-regulatory feedback loop that controls *flhDC* expression (Wozniak *et al*., 2009; Singer *et al*., 2013). Here, we report that RflM functions as an auxiliary protein that mediates specificity of RcsB to its target DNA and that a RcsB-RflM protein complex coordinately represses *flhDC* transcription.

Results

In a previous study we identified *rflM* as a repressor of flagellar master operon transcription that in turn is activated by $FlhD_4C_2$. The RflM-$FlhD_4C_2$ auto-regulatory feedback loop presumably allows *Salmonella* to fine-tune initiation of flagellar synthesis (Singer *et al*., 2013). We confirmed that the inhibitory effect of RflM on motility depended on the presence of the Rcs phosphorelay system (Wozniak *et al*., 2009), but not on other flagellar regulators like *lrhA*, *slyA*, *rtsB*, *fliZ* or the *hilD* operon (Supporting Information Fig. S1). RcsB is a previously described negative regulator of *flhDC*, and together with the LuxR-type auxiliary protein RcsA represses *flhDC* transcription in *E. coli* (Francez-Charlot *et al*., 2003). RflM also contains a LuxR-type helix-turn-helix DNA-binding motif at the C-terminus and RflM and RcsA of *Salmonella* Typhimurium display 80% amino acid sequence similarity (Supporting Information Fig. S2).

To test a putative link between RflM and RcsB in repression of *flhDC*, we performed an unbiased genetic screen using random transposon mutagenesis. The Tn10*d*Tc[*del-20*] transposon (T-POP) was introduced in a strain carrying a transcriptional *flhC-lac* reporter fusion and the *rflM* gene under control of the arabinose promoter resulting in deletion of the *araBAD* genes (Δ*araBAD921*::*rflM*$^+$ *flhC5213*::Mu*dJ*). This strain displayed an arabinose-dependent Lac$^-$ phenotype due to *rflM*-dependent repression of *flhDC*. Approximately 100,000 tetracycline-resistant colonies were screened for Lac$^+$ in the presence of arabinose (Ara-Lac$^+$) and three classes of Ara-Lac$^+$ colonies were identified by linkage analysis. One class of T-POP insertions were found to be near P_{araBAD}::*rflM*$^+$ and presumably resulted in an Ara-Lac $^+$ phenotype due to disruption of the *rflM* gene. A second class of T-POP transposons were linked to *rcsDBC* indicating disruption of the *rcsB* gene or other genes belonging to the RcsCDB phosphorelay system. The remaining T-POP insertions were neither linked to *rcsB*, nor to P_{araBAD}::*rflM*$^+$. We concluded that these transposon insertions disrupted other, previously described negative regulators of *flhDC* (Erhardt and Hughes, 2010; Mouslim and Hughes, 2014) and did not characterize them further. DNA-sequencing analysis of the three *rcsB*-linked T-POP insertion mutants revealed two insertions in the *rcsB* coding region and one insertion in the *rcsD* gene that is encoded upstream of *rcsB*. The transposon mutagenesis thus provided further evidence for a functional link between RcsB and RflM in repression of *flhDC*.

RcsB and RflM form a protein complex

We next employed bacterial-two-hybrid analysis to determine *in vivo* protein-protein interaction between truncated RcsB and RflM proteins lacking the respective C-terminal DNA-binding domains. Co-expression of RcsB and RflM fused to the bait plasmid pBT and the target plasmid pTRG (pBT-RcsB pTRG-RflM or pBT-RflM pTRG-RcsB) stimulated *lac* expression in a reporter strain in an inducer-concentration dependent manner (Fig. 1A). Transcription of the *lac* genes was not detected for control constructs and when RcsB (pBT-RcsB pTRG-RcsB) or RflM (pBT-RflM pTRG-RflM) were co-expressed, indicating that there is no self-interaction of RcsB or RflM under these conditions (Fig. 1B).

To investigate the stoichiometry of the RcsB-RflM protein complex, we performed size-exclusion chromatography followed by multiangle laser light-scattering (SEC-MALS) experiments (Wyatt, 1993; Tarazona and Saiz, 2003) (Fig. 2). Since RflM in the absence of RcsB was unstable and was not successfully purified alone, we co-purified His_6-SUMO-RflM/RcsB complex. The His_6-SUMO-RflM/RcsB protein complex eluted in one prominent peak with an apparent molecular mass of 57.96 kDa indicating a 1:1 stoichiometry based on the predicted molecular mass of the His_6-SUMO-RflM/RcsB complex of 58 kDa.

We next tested how RcsB influences RflM protein stability by analyzing protein levels of RflM. A functional, epitope-tagged RflM-HA construct was expressed from a chromosomal, arabinose-inducible promoter and protein levels were analyzed after inhibition of protein synthesis (Fig. 3A). RflM-HA protein degraded faster in a *rcsB* deletion mutant compared to wildtype, but no difference was observed upon *rcsB* overexpression. We next tested which protease was responsible for the rapid degradation of RflM (Fig. 3B). RflM-HA was expressed from its native promoter and protein levels were monitored after inhibition of *de novo* protein synthesis in various protease deletion backgrounds. We found that RflM-HA protein levels remained stable in *clpXP-lon* and

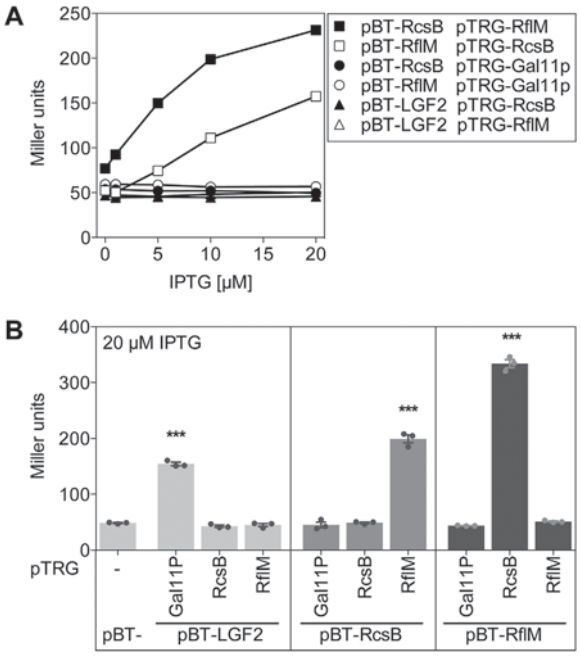

Fig. 1. RcsB and RflM interact in a bacterial-two-hybrid assay. *In vivo* protein-protein interactions between RcsB and RflM were determined using a transcription-based bacterial-two-hybrid assay of a *lacZ* reporter construct. RcsB and RflM lacking their DNA-binding domains were fused to λcI (pBT, bait plasmid) and α-RNA polymerase (pTRG, target plasmid), respectively.
A. Induction of *lacZ* transcription by interaction of RcsB-RflM was assessed at different IPTG inducer concentrations (0 μM, 1 μM, 5 μM, 10 μM, 20 μM) for pBT-RcsB pTRG-RflM (EM575, filled squares), pBT-RflM pTRG-RcsB (EM572, open squares), pBT-RcsB pTRG-Gal11P (EM577, filled circles), pBT-RflM pTRG-Gal11P (EM578, open circles), pBT-LGF2 pTRG-RcsB (EM579, filled triangles) and pBT-LGF2 pTRG-RflM (EM580, open triangles).
B. β-galactosidase activity of positive controls pBT-LGF2 pTRG-Gal11P (EM576), RcsB-RflM combinations (EM572, EM575), RcsB-RcsB and RflM-RflM self-interaction EM574 (pBT-RcsB pTRG-RcsB) and EM571 (pBT-RflM pTRG-RflM), vector controls EM577, EM578, EM579, EM580 and the empty vector EM567 was determined after induction with 20 μM IPTG. Bars represent mean values of three biological replicates. Individual data points are indicated and error bars represent the standard error of the mean. Asterisks indicate significant difference to the empty vector control according to Student's *t*-test (***$P < 0.0001$).

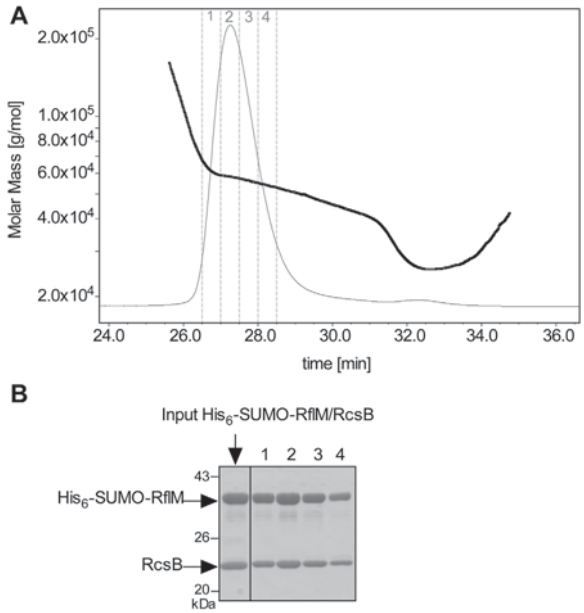

Fig. 2. Co-purified His_6-SUMO-RflM/RcsB proteins form a heterodimer.
A. SEC-MALS elution profile of purified His_6-SUMO-RflM/RcsB complex, as observed from the normalized MALS signals (gray line). The molar mass distribution, computed on the area between 25 and 35 min is shown in black. Elution fractions taken for SDS analysis are indicated with vertical lines.
B. SDS-polyacrylamide gel electrophoresis of SEC-MALS samples from elution fractions (1–4) of the His_6-SUMO-RflM/RcsB peak. His_6-SUMO-RflM (34 kDa) and RcsB (24 kDa) proteins are indicated with arrows.

lon deletion mutants, indicating that Lon is the main protease responsible for degradation of RflM.

RcsB-RflM complex coordinately represses flhDC *transcription*

We hypothesized that the interaction of RflM with RcsB could promote specificity of RcsB to its target DNA by formation of a stable RcsB-RflM protein complex that is able to efficiently repress *flhDC* transcription. To test for the specificity of RflM in promoting RcsB-dependent repression of *flhDC*, we analyzed the transcript levels of various RcsB targets in the absence or presence of *rflM* (Supporting Information Fig. S3). Target genes belonging to the RcsCDB regulon (*wzzB*, *dps* and *csgD*) were regulated by RcsB independently of the presence of RflM. In contrast, regulation of target genes belonging to the flagellar regulon (*flhC*, *aer* and *hilD*) was dependent on the presence of both RcsB and RflM.

We next analyzed the mode of action of the RcsB-RflM complex in repression of *flhDC* gene transcription using a transcriptional *flhC-lac* fusion. Expression of chromosomally-encoded *rflM* was controlled by an arabinose-inducible promoter (P_{araBAD}). It is important to note that $FlhD_4C_2$ is required for *rflM* expression (Singer *et al.*, 2013). Strains harboring the *flhC-lac* fusion do not produce a functional $FlhD_4C_2$ complex, and accordingly do not express *rflM* from its native promoter. Transcription of *flhC-lac* was reduced under conditions of *rflM* overexpression only in the presence of *rcsB* (Fig. 4B, compare columns 1 + 2 and 9 + 10). This demonstrated that RcsB is indispensable for the *rflM*-dependent repression of *flhDC*, which is consistent with previous observations (Wozniak *et al.*, 2009).

The role of RcsB in repression of *flhDC* expression was analyzed using several *rcsB* mutants. Overexpression of chromosomally-encoded *rcsB* from the anhydrotetracycline (ATc)-inducible P_{tetA} promoter resulted in

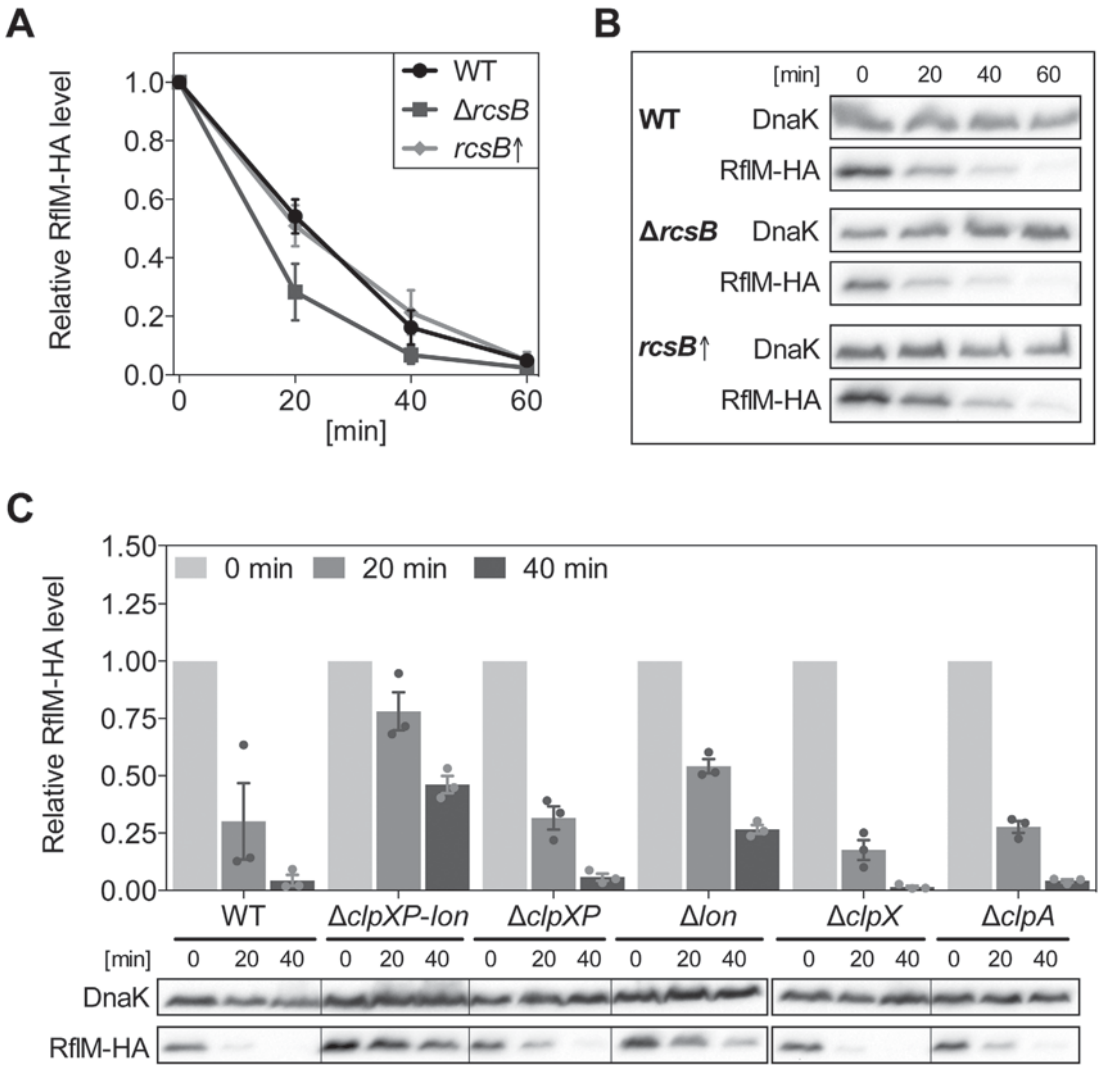

Fig. 3. RflM protein stability is affected by RcsB and Lon protease. RflM-HA protein levels were determined after stopping of protein synthesis in mutant strains to determine RflM stability. Protein samples were taken at indicated time points after inhibition of protein synthesis. Protein levels of each lane were normalized to the corresponding DnaK loading control level and reported relative to the $t = 0$ min sample.
A. RflM-HA protein levels after stopping of protein synthesis in absence of *rcsB* (Δ*rcsB*; dark gray line) or upon ATc-dependent *rcsB* overexpression (*rcsB*↑, light gray line) in comparison to a wildtype background (black line). All strains expressed RflM-HA from the arabinose-dependent P_{araBAD}-promoter. Data points represent mean values of three independent biological replicates. B. Representative immunoblots using anti-DnaK and anti-HA antibodies.
C. RflM-HA protein levels after stopping of protein synthesis in various protease deletion mutants (Δ*clpXP-lon*, Δ*clpXP*, Δ*lon*, Δ*clpX*, Δ*clpA*) in comparison to a wildtype background (WT). The RflM-HA fusion was expressed from the native promoter in all strains. Bars represent mean values of three independent biological replicates. Bottom: Representative anti-DnaK and anti-HA immunoblots.

decreased expression of *flhC-lac* (Fig. 4B, compare columns 1 and 3). However, *flhC-lac* transcription did not reach the repression level of *rflM* overexpression (Fig. 4B column 2). Chromosomal mutations of the RcsB phosphorylation site D56 resulted in a more active ($RcsB_{D56E}$, mimicking phosphorylation) or less active protein ($RcsB_{D56N}$, preventing phosphorylation) (Gupte *et al.*, 1997). We verified their functionality by motility analysis (Supporting Information Fig. S4). Motility of the $RcsB_{D56E}$ mutant was decreased, whereas motility of the $RcsB_{D56N}$ mutant was increased in comparison to the wildtype. In the absence of *rflM*, the phosphomimetic $RcsB_{D56E}$ mutant reduced *flhC-lac* transcription to the level observed under *rcsB* overexpression (Fig. 4B, compare columns 3 and 5). The phosphorylation-deficient $RcsB_{D56N}$ mutant did not affect *flhC-lac* expression in the absence of *rflM* (Fig. 4B, compare columns 1 and 7).

Coordinated overexpression of both *rcsB* and *rflM* from inducible promoters reduced *flhC-lac* expression to the level of *rflM* overproduction under wildtype *rcsB* levels (Fig. 4B, compare columns $1 + 2$ and $3 + 4$).

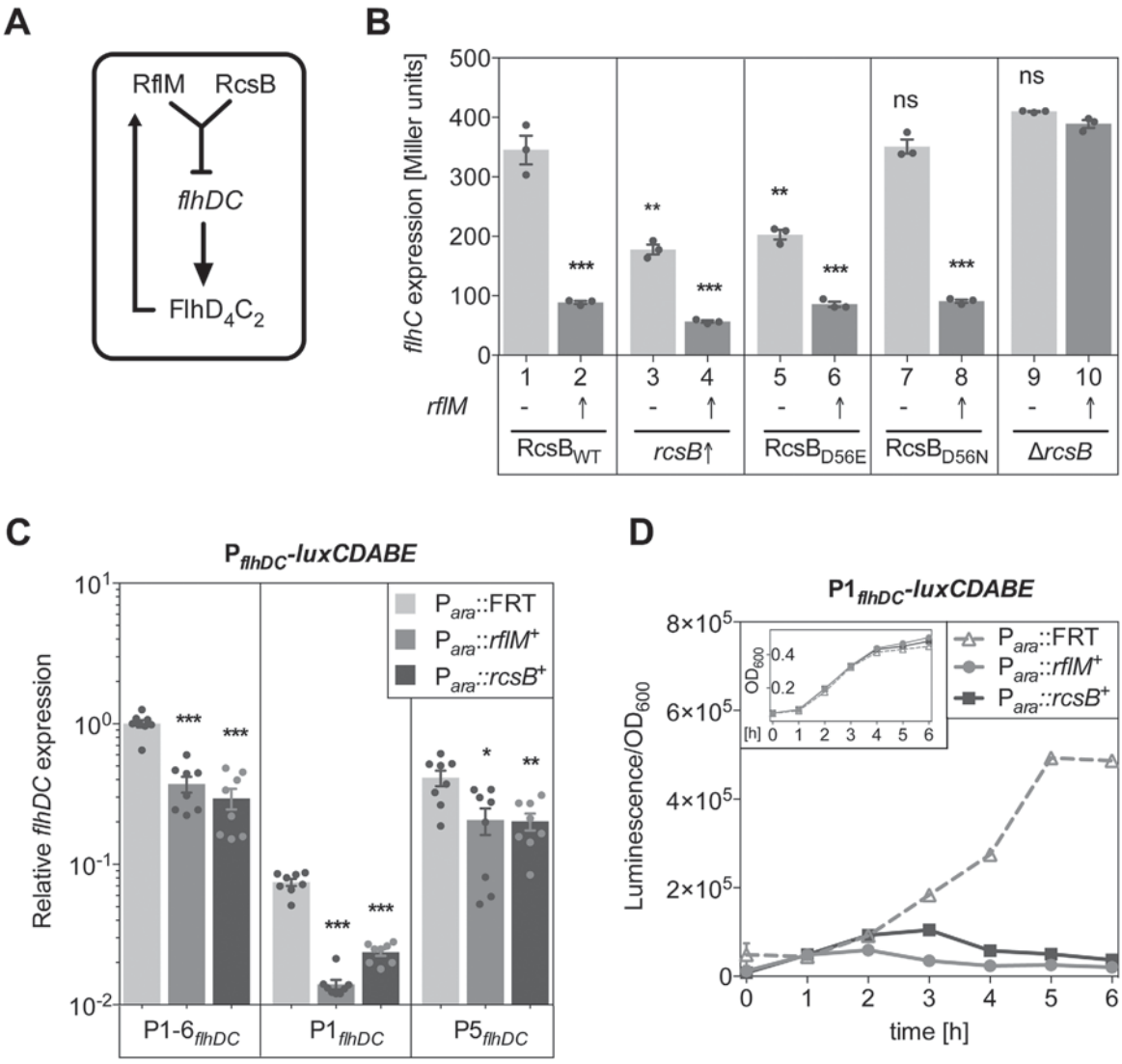

Fig. 4. Coordinated repression of *flhDC* transcription by RcsB and RflM.

A. Schematic regulatory model of repression of the flagellar master regulator *flhDC* by coordinated action of RcsB and RflM.

B. Expression of a transcriptional *flhC-lac* fusion upon chromosomal P_{araBAD}-dependent overexpression of *rflM* (*rflM*↑) in different *rcsB* mutant strains. Expression of *rflM* from its native promoter is $FlhD_4C_2$-dependent and the corresponding control strain (*rflM*$^-$) does not express *rflM* due to the transcriptional *flhC-lac* fusion. Chromosomal *rcsB* is either present as wildtype copy ($RcsB_{WT}$), overexpressed from the P_{tetA} promoter (*rcsB*↑), more active due to a mutation mimicking RcsB phosphorylation ($RcsB_{D56E}$), inactive due to a mutation preventing RcsB phosphorylation ($RcsB_{D56N}$) or absent due to a deletion of (Δ*rcsB*). Strains analyzed were EM517 (1; P_{araBAD}::FRT *flhC-lac rflM*$^-$), TH13069 (2; P_{araBAD}::*rflM*$^+$ *flhC-lac*), EM221 (3; P_{araBAD}::FCF *flhC-lac rflM*$^-$ P_{tetA}-*rcsB*), EM229 (4; P_{araBAD}::*rflM*$^+$ *flhC-lac* P_{tetA}-*rcsB*), EM2423 (5; P_{araBAD}::FRT *flhC-lac rflM*$^-$ $RcsB_{D56E}$), EM2426 (6; P_{araBAD}::*rflM*$^+$ *flhC-lac* $RcsB_{D56E}$), EM2424 (7; P_{araBAD}::FRT *flhC-lac rflM*$^-$$RcsB_{D56N}$), EM2427 (8; P_{araBAD}::*rflM*$^+$ *flhC-lac* $RcsB_{D56N}$), EM1432 (9; P_{araBAD}::FRT *flhC-lac rflM*$^-$ Δ*rcsB*), EM2486 (10; P_{araBAD}::*rflM*$^+$ *flhC-lac* Δ*rcsB*).

C. Relative *flhDC* expression level determined by measuring luminescence activity of a P_{flhDC}-*luxCDABE* fusion in *rflM* or *rcsB* overexpressing strains (P_{araBAD}::*rflM*$^+$ or P_{araBAD}::*rcsB*$^+$). To study expression from individual P_{flhDC} promoters P1 or P5, strains were used that retained only one functional promoter due to GTTGGT -10 box mutations of all other promoters. A duplication of the wildtype P_{flhDC}–*flhDC* (P_{flhDC}-*luxCDABE*-Km-P_{flhDC}–*flhDC*) allowed for expression of functional *flhDC* needed for activation of *rflM* transcription from the physiological P_{rflM} promoter. Samples were measured after 3 h incubation and were normalized to the corresponding P_{araBAD}::FRT control strain.

B + C. Bars represent mean values of at least three biological replicates. Individual data points are shown and error bars represent the standard error of the mean. Asterisks indicate significant difference to the control according to Student's *t*-test (ns, non-significant; $*P < 0.02$; $**P < 0.005$; $***P < 0.0001$).

D. Relative luminescence of $P1_{flhDC}$-*luxCDABE* fusion normalized to bacterial growth at OD_{600} upon *rflM* (P_{araBAD}::*rflM*$^+$; light-gray line) or *rcsB* (P_{araBAD}::*rcsB*$^+$; dark-gray line) overexpression. The inlay shows bacterial growth at OD_{600}. Symbols with connecting lines represent mean values of 10 biological replicates and error bars represent the standard error of the mean.

Notably, overexpression of *rflM* in the $RcsB_{D56N}$ strain restored the ability of RcsB to repress *flhC-lac*, suggesting that the presence of RcsB but not the phosphorylation status of RcsB is essential for RflM-mediated *flhDC* repression. Moreover, the results above indicated that *rcsB* overexpression bypassed the need for RcsB phosphorylation in repression of *flhDC* transcription. To exclude any possibility for phosphorylation of RcsB, we deleted the RcsCDB phosphorelay cascade. Overexpression of *rcsB* in absence of *rflM* retained the ability to repress *flhC-lac* to levels comparable upon overproduction of the phosphorylation-deficient $RcsB_{D56N}$ mutant (Supporting Information Fig. S5).

We next tested whether *rflM* expression was dependent on *rcsB* or vice versa. As shown in Supporting Information Fig. S6A, we observed no change in expression of a *rflM-lac* fusion when *rcsB* was overexpressed or deleted. Expression of *rflM* was analyzed in a strain that constitutively expressed *flhDC* from P_{tetA} to prevent any indirect effect of RcsB via *flhDC* repression. In addition, we did not observe changes in *rcsB-lac* expression upon *rflM* overproduction (Supporting Information Fig. S6B). Accordingly, we concluded that the inhibitory effect of RcsB and RflM on *flhDC* expression is due to their coordinated activity on the level of *flhDC* transcription. As described above, coordinated overexpression of *rcsB* and *rflM* resulted in a strong reduction of *flhDC* transcription. We next determined the change in *flhDC* expression under constant *rcsB* expression by simultaneous titration of *rflM* to analyze the cooperative repression. As shown in Supporting Information Fig. S6C, increasing levels of *rflM* decreased expression of *flhC-lac*, providing further evidence for a cooperative action of RflM and RcsB in repression of *flhDC*.

Originally, six transcriptional start sites of the *flhDC* promoter were described (annotated as P1 to P6) (Yanagihara *et al*., 1999). Recently, it was shown that only P1, P4, P5 and P6 are functional, but transcription of *flhDC* is primarily driven from the P1 and P5 promoters (Mouslim and Hughes, 2014). We determined which *flhDC* promoter is regulated via RcsB and RflM using *luxCDABE* fusions to *flhDC* promoter mutants that retained either a functional P1 or P5 promoter, respectively (Fig. 4C). We detected reduced *flhDC* expression for both promoter mutants under conditions of *rcsB* or *rflM* overproduction. Repression of the P1 promoter fusion was substantially greater than repression of the P5 promoter. Time-course analysis showed a continuous repression of *flhDC* under conditions of *rcsB* or *rflM* overexpression after entry in the early exponential phase (Fig. 4D). We thus concluded that the P1 promoter is the primary target for RcsB- and RflM-dependent *flhDC* repression.

RcsB-RflM protein complex binds to a RcsB box downstream of the P1 transcriptional start site of flhDC

A RcsB binding box has previously been predicted downstream of the P1 transcriptional start site of *flhDC* (Wang *et al*., 2007). To confirm the existence of the RcsB binding box and to test the hypothesis that RflM could stabilize binding of RcsB to the P1 promoter, we performed electrophoretic mobility shift assays (EMSA) with recombinant RcsB protein, phosphomimetic $RcsB_{D56E}$ and His_6-SUMO-RflM/RcsB protein complex (Fig. 5).

We observed binding of purified RcsB protein to a DNA fragment of the complete P_{flhDC} promoter region (−560 to −90 nucleotides upstream ATG). A control DNA fragment (*gyrA*) was not shifted, indicating specific binding of RcsB to the *flhDC* promoter. RcsB protein bound also weakly to the $P1_{flhDC}$ promoter fragment containing the annotated RcsB box (−271 to −71 nucleotides upstream ATG), but not to DNA fragments containing the $P4/6_{flhDC}$ (−431 to −231 nucleotides upstream ATG) or $P5_{flhDC}$ (−588 to −388 nucleotides upstream ATG) promoter regions (Fig. 5A and B, left column). The phosphomimetic $RcsB_{D56E}$ mutant showed higher binding affinity to P_{flhDC} and $P1_{flhDC}$ promoter fragments, but also weak binding to $P4/6_{flhDC}$ and $P5_{flhDC}$ DNA fragments indicating reduced target specificity (Fig. 5B, right column).

Purified His_6-SUMO-RflM/RcsB protein complex bound to a DNA fragment containing the complete *flhDC* promoter, as well as to a DNA fragment containing the $P1_{flhDC}$ promoter with apparent higher affinity than RcsB or $RcsB_{D56E}$ (Fig. 5B, middle column). His_6-SUMO-RflM/RcsB protein complex formed an additional protein-DNA species that was not observed in reactions containing RcsB or $RcsB_{D56E}$ (Fig. 5B, middle column, highlighted by arrows). This faster migrating protein-DNA complex might be due to a tighter interaction of His_6-SUMO-RflM/RcsB complex to its target DNA. We did not observe binding of His_6-SUMO-RflM/RcsB complex to a control DNA fragment or DNA fragments containing the $P4/6_{flhDC}$ and $P5_{flhDC}$ promoter regions. Samples of purified RcsB, $RcsB_{D56E}$ and His_6-SUMO-RflM/RcsB complex used for the EMSA experiments contained comparable levels of RcsB protein as determined by SDS-PAGE analysis (Fig. 5C). It is important to note that the used His_6-SUMO-RcsB and His_6-SUMO-RflM/RcsB fusion constructs retained the ability to repress *flhC-lac* transcription *in vivo* (Supporting Information Fig. S7). We also detected *in vivo* activity for the His_6-SUMO-RflM fusion in the presence of chromosomally-encoded *rcsB*.

To test if the helix-turn-helix (HTH) DNA-binding domain of RflM is required for RcsB/RflM-dependent repression of *flhDC* and binding to the *flhDC* promoter,

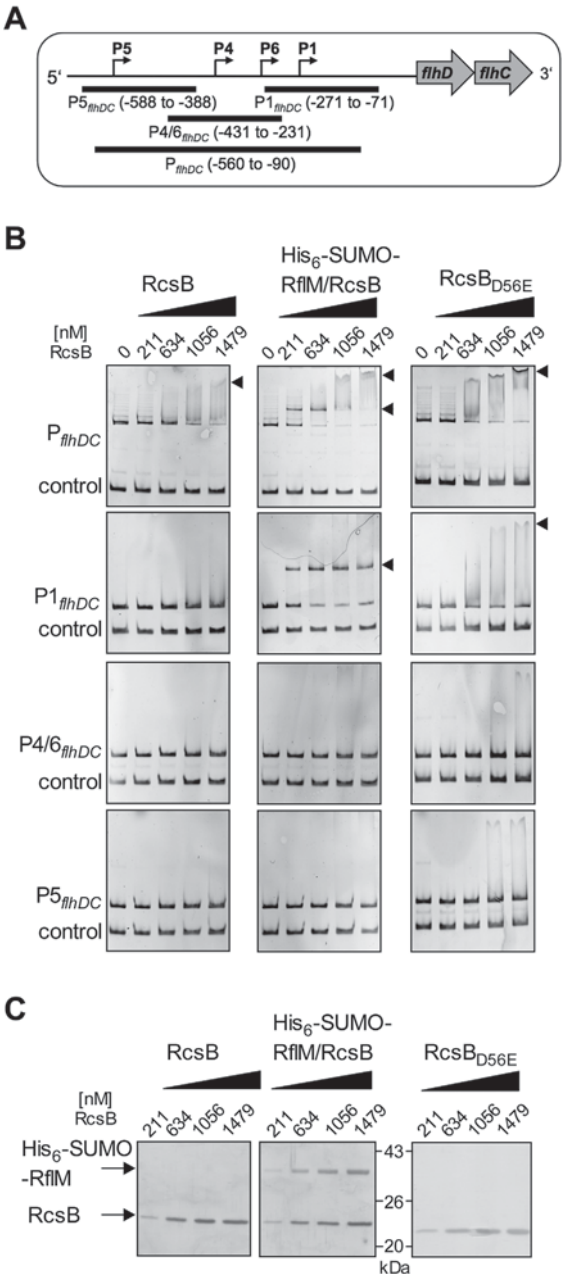

Fig. 5. Purified RcsB-RflM complex binds with high affinity to the *flhDC* promoter.
A. Schematic representation of the P_{flhDC} promoter region. Transcriptionally active start sites P1, P4, P5 and P6 that are involved in *flhDC* transcription are highlighted (Kröger *et al.*, 2013). Promoter fragments used for electrophoretic mobility shift assays (EMSA) are indicated and the respective positions relative to the ATG start codon of *flhD* are given in brackets.
B. EMSA of P_{flhDC} promoter fragments with increasing amounts of purified RcsB protein, $RcsB_{D56E}$ phosphomimetic mutant or purified His_6-SUMO-RflM/RcsB complex. Samples were adjusted to equal RcsB concentrations and incubated with 100 ng *flhDC* promoter DNA and negative control DNA (*gyrA*). Arrowheads indicate protein-DNA complexes.
C. SDS-polyacrylamide gelelectrophoresis of RcsB, $RcsB_{D56E}$ and His_6-SUMO-RflM/RcsB samples used for EMSAs. RcsB concentrations are indicated and His_6-SUMO-RflM (34 kDa) and RcsB (24 kDa) are highlighted with arrows.

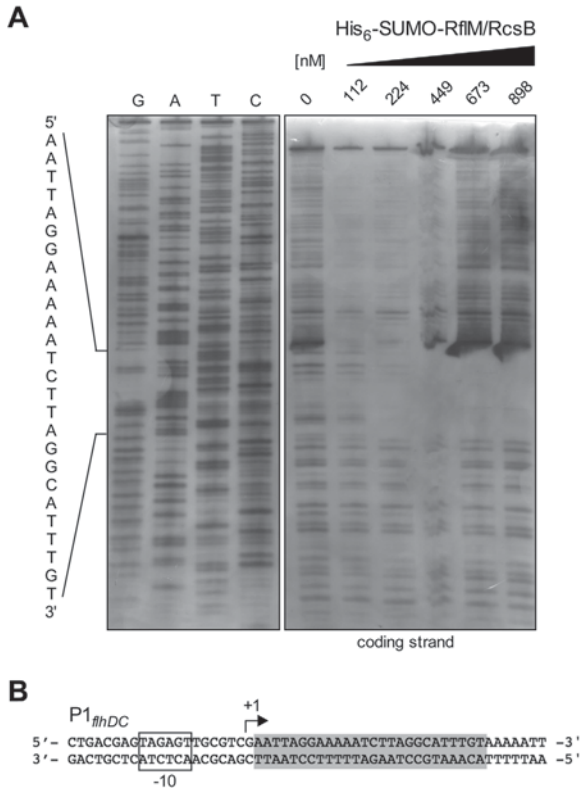

Fig. 6. Determination of His_6-SUMO-RflM/RcsB binding site by DNaseI footprint.
A. DNaseI footprint analysis of 5′-DIG-labeled $P1_{flhDC}$ promoter fragment in the presence of increasing amounts of purified His_6-SUMO-RflM/RcsB complex. The $P1_{flhDC}$ region protected from DNaseI digestion is indicated and the sequence represents the identified RcsB/RflM binding site. The sequencing reactions of the $P1_{flhDC}$ promoter DNA fragment are shown in lanes G, A, T, C.
B. DNA sequence of the *flhDC* promoter comprising the P1 promoter and the His_6-SUMO-RflM/RcsB binding site (highlighted in gray). The P1 transcriptional start site (+1) and −10 box are indicated.

we analyzed the function of a RflM mutant lacking its HTH domain. Both the exchange with the HTH domain of the *Salmonella* LuxR-homolog SdiA and the deletion of the HTH domain prevented repression of *flhC-lac* transcription (Supporting Information Fig. S8A). To confirm that RflM deleted for its HTH domain is expressed and stable, we purified His_6-SUMO-RflM(ΔHTH)/RcsB complex. Recombinant His_6-SUMO-RflM(ΔHTH)/RcsB complex showed only weak binding to $P1_{flhDC}$ in EMSA (Supporting Information Fig. S8B), indicating that the DNA-binding domain of RflM is indispensable to mediate repression of *flhDC* by the RcsB-RflM complex.

We next performed a DNaseI protection assay with 5′-digoxigenin labeled $P1_{flhDC}$ promoter fragment in the presence of His_6-SUMO-RflM/RcsB protein complex to validate the predicted RcsB box downstream of the P1 transcriptional start site of *flhDC*. As shown in Fig. 6A,

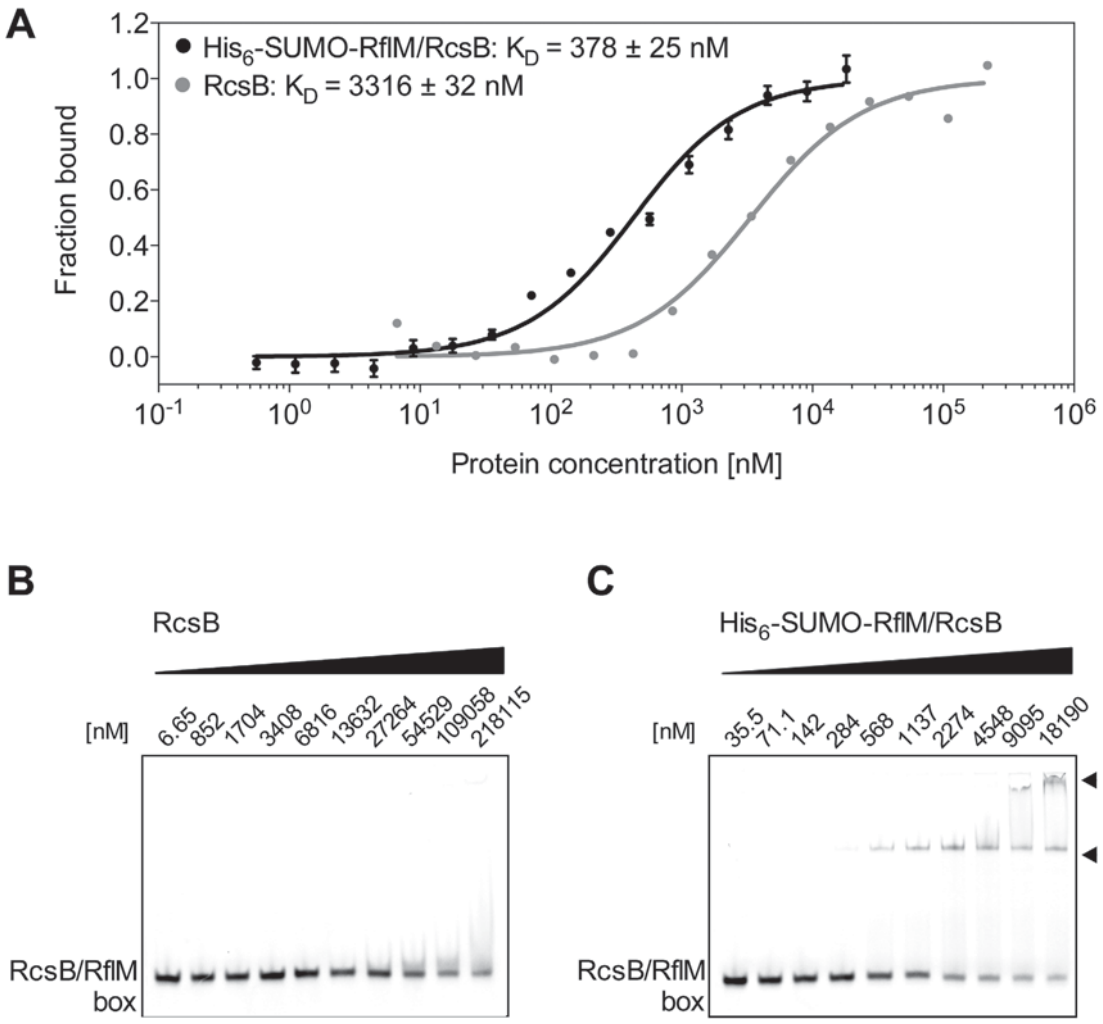

Fig. 7. Binding kinetics of purified RcsB and RcsB-RflM complex.
A. Dose response curve of the binding of RcsB protein (gray) and His_6-SUMO-RflM/RcsB complex (black) to the RcsB/RflM binding site of the *flhDC* promoter determined using microscale thermophoresis (MST). Individual data points with error bars representing standard deviation and the curve fit of three technical replicates of a representative experiment are shown.
B and C. EMSA of MST samples with 5′-Cy5-labeled DNA and RcsB or His_6-SUMO-RflM/RcsB complex, respectively. Arrowheads indicate protein-DNA complexes.

we identified a region corresponding to nucleotides +2 to +27 downstream of the +1 transcriptional start site of the P1 *flhDC* promoter that was protected from DNaseI degradation by increasing amounts of His_6-SUMO-RflM/RcsB complex. This region contained the predicted RcsB box (nucleotides +5 to +19) (Fig. 6B).

RflM enhances binding affinity of RcsB to the flhDC *target promoter DNA*

Using microscale thermophoresis (MST) we next determined binding kinetics of purified RcsB protein and His_6-SUMO-RflM/RcsB protein complex to the identified RcsB/RflM binding box. We detected increased fluorescence of 5′-Cy5-labeled *flhDC* promoter DNA with increasing concentrations of RcsB or His_6-SUMO-RflM/RcsB complex due to enhancement of fluorescence intensity after DNA-binding (Fig. 7). The measured fluorescence intensities after protein denaturation were comparable (< 15% difference), which confirmed the specificity of the binding. The dissociation constant of His_6-SUMO-RflM/RcsB complex ($K_D = 378 \pm 25$ nM) was approximately tenfold lower than for RcsB protein alone ($K_D = 3316 \pm 32$ nM) demonstrating higher affinity of RcsB-RflM complex to the RcsB/RflM binding box (Fig. 7A). The higher binding affinity of His_6-SUMO-RflM/RcsB compared to RcsB protein was confirmed by gel shift analysis of the MST samples (Fig. 7B and C).

In summary, our results demonstrate that RflM protein promotes RcsB target specificity for repression of *flhDC*

transcription by formation of a stable RcsB-RflM complex, which enables the RcsB/RflM complex to bind to the RcsB/RflM box of the $P1_{flhDC}$ promoter with enhanced efficiency.

Discussion

Regulation of flagellar synthesis is controlled by the RcsCDB phosphorelay system in both *E. coli* and *S. enterica* serovar Typhimurium. In *E. coli*, it has been shown that an auxiliary regulatory protein, RcsA, enhances RcsB-dependent repression of *flhDC* (Francez-Charlot *et al*., 2003). In *Salmonella*, however, RcsB-mediated regulation of the flagellar master operon *flhDC* has been described to be independent from RcsA (Wang *et al*., 2007). RcsA, the auxiliary co-regulator of RcsB, is conserved in many *Enterobacteriaceae* species, such as *E. coli, Salmonella* Typhimurium and Typhi, *Yersinia* spp., *Shigella flexneri* and *Erwinia* spp. (Huang *et al*., 2006). RcsA enhances RcsB-dependent capsule synthesis by binding together with RcsB to the RcsAB box of target genes (Majdalani and Gottesman, 2005). Beside RcsA, several other RcsB co-regulators are implicated in regulation of a range of different target genes. In *E. coli*, RcsB regulates together with the auxiliary proteins GadE and BglJ acid stress resistance and the global regulators H-NS, LeuO and CRP, respectively, (Castanié-Cornet *et al*., 2010; Salscheider *et al*., 2014). In *Salmonella* Typhi, RcsB regulates together with TviA the synthesis of the capsular polysaccharide Vi antigen (Virlogeux *et al*., 1996).

Previous studies also suggested a role of the RcsCDB system in auto-regulation of the flagellar master regulatory operon *flhDC* in *Salmonella*. Auto-regulation of *flhDC* involves expression of a $FlhD_4C_2$-dependent repressor, *rflM* (Wozniak *et al*., 2009; Singer *et al*., 2013). The flagellar-specific regulator RflM is conserved among *Enterobacteriaceae* and shares high sequence similarity to RcsA. RcsB, as well as RcsA and RflM contain a LuxR-type C-terminal helix-turn-helix DNA-binding domain (Henikoff *et al*., 1990).

In the present study, we elucidated the mode-of-action of RcsB and RflM in regulation of *flhDC*. We demonstrate that RflM functions as a novel co-regulator of RcsB and mediates target specificity of unphosphorylated RcsB for repression of *flhDC*. RcsB and RflM form a heterodimeric complex that coordinately represses *flhDC* transcription by binding to the RcsB/RflM box downstream of the P1 transcriptional start site of the *flhDC* promoter region. Overexpressed RcsB or a phosphomimetic $RcsB_{D56E}$ mutant were able to repress *flhDC*, but RcsB-mediated repression of *flhDC* increased significantly in the presence of RflM. RflM, however, did not repress *flhDC* transcription in the absence of RcsB protein. It has been shown previously that RflM protein levels decline rapidly after reaching a maximum during early logarithmic growth (Mouslim and Hughes, 2014). We showed that RflM is unstable under conditions where interaction with RcsB is not possible and that RflM is subjected to Lon-dependent proteolytic degradation, similar to what has been reported for RcsA (Stout *et al*., 1991). In support of the requirement of RcsB for RflM stability, we were not able to purify RflM protein without co-expression of RcsB.

It has been shown previously that RcsB binds to target DNA as a homodimer or as a heterodimer together with auxiliary co-regulators (Majdalani and Gottesman, 2005). We did not detect self-dimerization of either RcsB or RflM in our experiments. The lack of self-dimerization could be due to the absence of target DNA or phosphorylation of RcsB that presumably would facilitate RcsB dimer formation in the absence of RflM. However, we detected interaction between RcsB and RflM resulting in formation of a stable RcsB-RflM heterodimeric complex as determined using SEC-MALS analysis. We propose that RflM stabilizes RcsB binding to the *flhDC* promoter leading to formation of a stable RcsB-RflM heterodimer and thereby enhances target specificity of the RcsB-RflM complex to the binding site within the *flhDC* promoter independent of the phosphorylation state of RcsB.

As mentioned, we found that phosphorylation of RcsB was not essential for repression of *flhDC* in the presence of RflM, but for RcsB-mediated repression of *flhDC* in the absence of RflM. These results indicated that RflM directs RcsB to specifically repress *flhDC* gene transcription independently of external stimuli that would result in RcsB phosphorylation, similar to the mode of action of other RcsB co-regulator complexes such as BglJ-RcsB (Venkatesh *et al*., 2010).

We next analyzed binding of RcsB-RflM complex to the *flhDC* promoter in detail and found that purified RcsB-RflM complex bound to DNA containing the P1 *flhDC* transcriptional start site. Purified RcsB protein alone bound with tenfold lower affinity to a promoter fragment containing the P1 transcriptional start site in comparison to purified RcsB-RflM complex. Likewise, the purified phosphomimetic RcsB mutant ($RcsB_{D56E}$) bound with lower affinity and additionally showed reduced target specificity compared to wildtype RcsB. This result indicated that the activated RcsB variant bound to DNA unspecifically. In support of this, transcription from the $P5_{flhDC}$ promoter was slightly reduced upon *rcsB* or *rflM* overexpression, although we detected no binding of the RcsB-RflM complex to a promoter fragment containing the P5 transcriptional start site. Beside unspecific effects this could be due to indirect repression of *hilD* via RcsB/RflM as described before

(Mouslim and Hughes, 2014). We further demonstrated that efficient binding of the RcsB-RflM complex to the *flhDC* promoter required the DNA-binding domain of RflM. We thus propose that RflM modulates binding affinity of RcsB for its target DNA and enables a fast and stable binding of a RcsB-RflM heterodimer to the *flhDC* promoter.

The binding sequence of RcsB in target promoter DNA (RcsB box) is conserved throughout enteric bacteria and is also present in the *flhDC* promoter of *E. coli* and *S. enterica* (Wehland and Bernhard, 2000; Francez-Charlot *et al.*, 2003). We confirmed binding of RcsB-RflM protein complex to a putative RcsB box downstream of the P1 transcriptional start site by DNaseI protection assay, EMSA and microscale thermophoresis. Binding of RcsB-RflM complex was specific to *flhDC* promoter fragments containing the RcsB/RflM box and we did not detect binding to other fragments of the *flhDC* promoter. This is consistent with previously isolated suppressor mutations that relieved RflM-mediated inhibition of motility, which were limited to a region comprising the RcsB box downstream of the P1 promoter (Wozniak *et al.*, 2009).

In summary, we propose here a new regulatory mechanism for the control of flagellar synthesis in response to environmental stimuli and growth phase (Fig. 8). Various environmental signals might activate the RcsCDB phosphorelay cascade and result in phosphorylation of RcsB. Phosphorylated RcsB would be able to repress *flhDC* with low affinity by binding to the RcsB box in the *flhDC* promoter region as a homodimer. In the absence of activating environmental signals and during early logarithmic growth, *rflM* is activated by an initial surge of *flhDC* expression. RflM would then be able to subsequently direct an existing pool of unphosphorylated RcsB to its target DNA downstream of the $P1_{flhDC}$ promoter resulting in high affinity binding of a RcsB-RflM heterodimer and repression of *flhDC* operon transcription.

We propose that *Salmonella* adapted the specificity of the existing, global RcsCDB regulatory system by evolving a flagellar-specific auxiliary protein, RflM. The $FlhD_4C_2$-dependent RflM protein thus enables *Salmonella* to fine-tune expression levels of the motility master regulator during early stages of flagellar synthesis by sequestering RcsB protein for repression of flagellar synthesis independent on the presence of external stimuli.

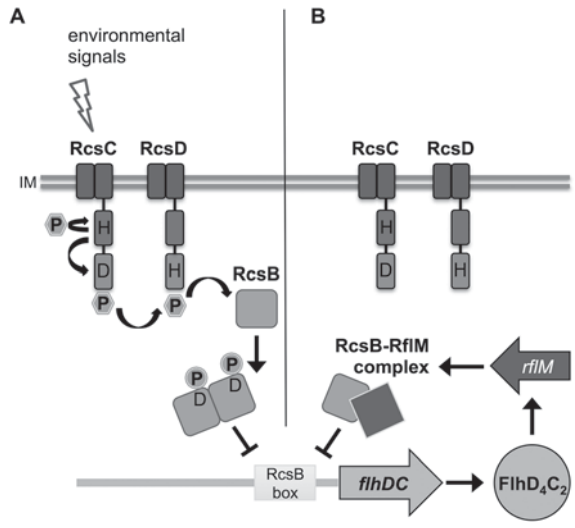

Fig. 8. Schematic model of RcsB-RflM-dependent regulation of *flhDC* transcription.
A. Environmental signals activate the RcsCDB phosphorelay, which results in autophosphorylation of RcsC and subsequent transfer of the phosphoryl group via RcsD to RcsB. Phosphorylated RcsB is able to bind as homodimer with low affinity to the RcsB box in the *flhDC* promoter region.
B. In the absence of environmental signals, phosphorylation of RcsB does not occur. RflM expression is activated by induction of flagellar synthesis during early growth phase. RflM interacts with RcsB and forms a heterodimer that binds to the RcsB/RflM box of *flhDC* with high affinity to repress *flhDC* transcription after the initial surge of *flhDC* expression.

Experimental procedures

Bacterial strains, plasmids and media

All bacterial strains used in this study are listed in Supporting Information Table S1. pSUMO harboring Ulp1-cleavable His_6-SUMO tag (Andréasson *et al.*, 2008) was used for protein overexpression. *rcsB* and *rflM* were PCR-amplified from genomic DNA of *S. enterica* serovar Typhimurium strain LT2. N-terminal His_6-SUMO fusions to RcsB and RflM were made via *Bsa*I/*Hind*III. For the His_6-SUMO-RflM/RcsB complex, *rcsB* was cloned into His_6-SUMO-RflM via *Hind*III/*Xho*I by addition of a ribosomal binding site (RBS; AAGAAGGAGATATACAT) resulting in His_6-SUMO-RflM-RBS-RcsB. pTRG and pBT (Dove and Hochschild, 2004) were used for protein-protein interaction studies. RcsB and RflM lacking the respective DNA-binding domains were cloned into pTRG and pBT via *Not*I/*Xho*I resulting in N-terminal fusions to the N-terminal domain of the α-subunit of *E. coli* RNA polymerase (α-NTD) and the phage λ-cI DNA-binding protein, respectively. Chromosomal amino acid mutations ($RcsB_{D56E}$ and $RcsB_{D56N}$) and helix-turn-helix domain changes in *rflM* (P_{araBAD}::*rflM*(*sdiA*-HTH), P_{araBAD}::*rflM*(ΔHTH)) were constructed using the λ-RED recombination system with pKD46 as described previously (Karlinsey, 2007). N-terminal HA-tagging of RflM in the chromosome was performed according the method of Uzzau *et al.* (2001). *S. enterica* serovar Typhimurium and *E. coli* strains were cultivated in lysogeny broth (LB) (Bertani, 2004) at 37°C, supplemented with ampicillin (100 μg ml^{-1}), chloramphenicol (12.5 μg ml^{-1}), kanamycin (50 μg ml^{-1}) or tetracycline (15 μg ml^{-1}) if needed. To induce P_{araBAD} or P_{tetA} dependent gene expression, cultures were supplemented with 0.2% arabinose or 1 μg ml^{-1} anhydrotetracycline, respectively. Motility agar was prepared as described before (Gillen and Hughes, 1991). The generalized transducing phage of *S. enterica* servovar Typhimurium P22 *HT105/1 int-201* was used in all transductional crosses (Sanderson and Roth, 1988).

Isolation of random T-POP insertions

Chromosomal T-POP transposon insertions were generated in strain EM423 (Δ*araBAD921*::*rflM*$^{+}$ *flhC5213*::Mu*dJ*) containing plasmid pNK2880 that constitutively expressed the Tn10 transposase with altered transposition sequences as described before (Singer *et al*., 2013). Strain EM423 expressed *rflM* from the chromosomal arabinose promoter P_{araBAD} and harbored a chromosomal *flhC-lac* transcriptional reporter fusion (*flhC5213*::Mu*dJ*). In the presence of arabinose, strain EM423 was Lac^{-} due to repression of *flhC-lac* reporter transcription by *rflM* (Singer *et al*., 2013). Random T-POP insertions were introduced by P22 phage from donor TH3466 (LT2 F'128 (pro-lac) *zzf382*::Tn*10d*Tc[*del-20*] proAB47) (Bender and Kleckner, 1992). About 100,000 T-POP insertions were screened for loss of *rflM*-dependent *flhDC* repression resulting in an Ara-Lac^{+} phenotype in the presence of tetracycline. 87 Ara-Lac^{+} T-POP insertions were isolated and further characterized as described in Results.

Motility assay

For quantification of swimming motility, motility agar plates were inoculated with overnight cultures of at least 3 independent biological replicates and incubated 4 h at 37°C. The diameter of the swimming halo was measured using the software NIH ImageJ64 1.47v and normalized to the wildtype.

β-galactosidase assay

β-galactosidase activity of at least three independent biological replicates was determined in mid-exponential growth phase as described previously (Singer *et al*., 2013).

Bacterial-two-hybrid assay

In vivo protein-protein interaction studies were performed with a transcription-based bacterial-two-hybrid system as described by Dove and Hochschild (2004). Briefly, overnight cultures of three independent biological replicates of the *E. coli* BacterioMatch reporter strain harboring the pTRG target and pBT bait plasmids fused to the proteins of interest were grown in LB medium supplemented with 0–20 μM isopropyl-β-$_{D}$-thiogalactopyranoside (IPTG) for induction of fusion proteins. Samples were diluted 1:100 in LB medium supplemented with the same IPTG concentration as used for the overnight cultures and grown to mid-exponential phase. Protein-protein interactions stabilized binding of RNA polymerase to a promoter driving *lacZ* reporter transcription and β-galactosidase activity was quantified as described. pTRG-Gal11P and pBT-LGF2 (Stratagene) served as controls for the two-hybrid interaction.

Protein stability assay

Protein stability was determined and visualized by immunoblotting as described previously (Aldridge *et al*., 2006; Mouslim and Hughes, 2014) with the following modifications. Briefly, 1:100 dilutions from overnight cultures were grown to mid-exponential phase and protein synthesis was stopped by addition of 12.5 μg ml^{-1} chloramphenicol and 0.5 mg ml^{-1} spectinomycin. Total protein extracts were collected from 1 ml culture at 0, 20, 40 and 60 min after stopping of protein synthesis, enriched by precipitation with 10% Trichloroacetic acid (TCA) and resuspended in SDS sample buffer. 100 OD-units were subjected to SDS-PAGE analysis followed by immunoblotting on polyvinylidene difluoride (PVDF) membranes (Biorad). To expose potentially buried epitope tags, membranes were stripped with 62.5 mM Tris, 2% SDS and 100 mM β-mercaptoethanol before probing. Proteins were detected using anti-HA (mouse, Covance) and anti-DnaK (mouse, Abcam) antibodies. Protein bands were quantified using the software NIH ImageJ64 1.47v.

RNA isolation and quantitative real-time PCR

Total bacterial RNA was isolated from mid-exponential phase cultures using the RNeasy mini kit (Qiagen). Genomic DNA was removed from purified RNA using the TURBO DNA-free kit (Ambion). The SensiFast SYBR No-ROX One Step kit (Bioline) was used for reverse transcription and quantitative real-time PCR (qRT-PCR) analysis in a Rotor-Gene Q lightcycler (Qiagen). Target gene mRNA transcript levels were normalized to the geometric mean of reference genes (*gyrB*, *gmk* and *rpoD*) and relative changes in transcript levels were determined according to the ΔΔCT method of Pfaffl (2001).

Luminescence assay

Luminescence activity of luciferase reporter strains was determined in a Varioscan microplate reader for four independent biological replicates. Briefly, 1:100 dilutions from overnight cultures were grown in 96-well microtiter plates in LB supplemented with 25 μg ml^{-1} kanamycin to retain the P_{flhDC}-*luxCDABE*-Km^{+}-P_{flhDC} promoter duplication and 0.2% arabinose for overexpression of genes under control of the arabinose promoter P_{araBAD}. Bacterial growth was determined by measuring absorbance at 600 nm and relative luminescence was determined after normalization to the growth.

Purification of RcsB, $RcsB_{D56E}$ and His_6-SUMO-RflM/RcsB complex

For overexpression of His_6-SUMO-RcsB, His_6-SUMO-$RcsB_{D56E}$ and His_6-SUMO-RflM-RBS-RcsB, cultures were grown at 37°C with shaking at 200 rpm until mid-exponential phase and protein expression was induced for three hours by addition of 0.2 mM IPTG. Soluble His_6-SUMO-RcsB, His_6-SUMO-$RcsB_{D56E}$ and His_6-SUMO-RflM/RcsB complex were purified using Talon Superflow (GE Healthcare) under native conditions. Purified His_6-SUMO-RcsB and His_6-SUMO-$RcsB_{D56E}$ was supplemented with recombinant produced His_6-Ulp1 protease and dialyzed overnight at 4°C. Contaminants (His_6-Ulp1, His_6-SUMO and uncut His_6-SUMO-RcsB or His_6-SUMO-$RcsB_{D56E}$) were removed by binding to Ni-nitrilotriacetic acid (NTA) agarose

(Protino; Macherey-Nagel). Afterwards, proteins were concentrated using Vivaspin 6 concentrators (Sartorius Stedim) and subjected to gel filtration using a Superdex 200 10/300 GL column (GE Healthcare). Major peak fractions were merged and used for further analysis.

SEC-MALS

For molecular mass determination of the His_6-SUMO-RflM/RcsB complex, we performed an inline SEC (Äkta PURE, GE Healthcare) coupled with a MALS detector (miniDAWN TREOS, Wyatt Technology) and a differential refractometer (RI) (Optilab T-rEX, Wyatt Technology). The latter was used to calculate the effective complex concentration, by using a standard protein refractive index increment value of 0.185 ml g^{-1}. The protein separation was achieved using a Superdex 200 Increase 10/300 GL column (GE Healthcare) with a 0.5 ml min^{-1} flow rate. To obtain the molecular weight (MW) of the eluted proteins we analyzed the obtained RI and MALS signals recorded at three angles by means of the ASTRA 6 software (Wyatt Technology).

EMSA

DNA fragments were PCR-amplified from genomic DNA of *Salmonella* Typhimurium strain LT2 using the following oligonucleotides: P_{flhDC} (5′-TTTAACAGCGGAGGGCGTAT-3′ and 5′-CATAGCAGCGCTCAGACATT-3′), $P1_{flhDC}$ (5′-TCACATATTTTCTAAAATCGCC-3′ and 5′-GAAGCAAAAAGGTCAAATGC-3′), $P4/6_{flhDC}$ (5′-CGTTATTTTAACAGAGAGAAAC-3′ and 5′-CATACAACGGAGCGGGAC-3′), $P5_{flhDC}$ (5′-GCTAAAAGTTAAATCAAATGAGC-3′ and 5′-GTCAACACCAAATTCTTTTTTG-3′) and *gyrA* (5′-ATGAGCGACCTTGCGAGAG-3′ and 5′-GCGCACGGCCAACAATGACC-3′). Binding reactions using 100 ng *flhDC* promoter DNA, 100 ng competitor DNA *gyrA* and increasing amounts of purified RcsB, $RcsB_{D56E}$ or His_6-SUMO-RflM/RcsB complex were carried out for 20 min at room temperature in binding buffer (10 mM Tris-HCl pH 7.5, 50 mM KCl, 1 mM DTT). Samples were separated on 7% Tris-borate-EDTA (TBE) polyacrylamide gels and DNA was visualized after ethidiumbromide-staining with a CCD camera (Biorad).

DNaseI footprinting

The $P1_{flhDC}$ DNA fragment comprising the putative RcsB/RflM binding site was digoxigenin (DIG)-labeled on the coding strand using a 5′-DIG-labeled primer (5′-DIG-TCACATATTTTCTAAAATCGCC-3′). Sequencing reactions were performed using the USB Thermo Sequenase cycle sequencing kit (Affimetrix). Binding reactions with 100 ng DIG-labeled *flhDC* promoter DNA and increasing amounts of His_6-SUMO-RflM/RcsB complex were performed as described above and followed by subsequent DNaseI (Roche) treatment. Stopping solution (10 mM EDTA, 10 μg ml^{-1} yeast tRNA) was added, DNA was recovered using phenol-chloroform extraction and separated on 6% TBE-7 M urea polyacrylamide gels with subsequent transfer to a Nytran nylon membrane (GE Healthcare) and UV crosslinking. DIG-labeled DNA was detected using CDP-Star (Roche) and the anti-DIG-alkaline phosphatase antibody (Fab fragments; Roche).

MST

The RcsB/RflM binding site (−204 to −174 relative to ATG) was Cy5-labeled on the coding strand using a 5′-Cy5-labeled primer (5′-Cy5-CGAATTAGGAAAAATCTTAGGCATTTGTAA) and duplexed with a complementary primer. Binding reactions using 100 nM 5′-Cy5-labeled DNA and serial dilutions of purified RcsB or His_6-SUMO-RflM/RcsB were performed as described above. Prior dilution, protein samples were centrifuged 10 min at high speed to remove aggregates. Samples were loaded into standard capillaries and measured on a Monolith NT.115 (Nanotemper) with 15% LED and 20% MST power. For testing of fluorescence intensities under SDS-denaturing conditions, samples were mixed with 2x SD mix (4% SDS, 40 mM DTT), incubated 5 min at 95°C and loaded into standard capillaries for fluorescence measurement. Dissociation constants K_D were determined using MO.Affinity Analysis V.2.1.2 software (Nanotemper) from fluorescence changes as described previously (Baaske *et al.*, 2010). MST samples were subjected to 7% TBE polyacrylamide gels and 5′-Cy5-labeled DNA was detected using a Typhoon™ FLA900 Bioscanner (GE Healthcare).

Acknowledgements

We are grateful to Hagen Richter for help with the analytical gel filtration, Kelly T. Hughes for generous strain donation and constant support, Nadine Körner for expert technical assistance and members of the Erhardt lab for useful discussions of the manuscript. This work was funded by the Helmholtz Association Young Investigator grant number VH-NG-932 (to M.E.), VH-NG-727 (to A.S.), the People Programme (Marie Curie Actions) of the Europeans Unions' Seventh Framework Programme grant number 334030 (to M.E.) and the Leibniz University Hannover (to L.C. and T.C.). C.K. gratefully acknowledges support by the President's Initiative and Networking Funds of the Helmholtz Association of German Research Centers (HGF) under contract number VH-GS-202. H.M.S. acknowledges scholarship support of the Boehringer Ingelheim Fonds.

The authors declare no conflict of interest.

References

Aldridge, P., Karlinsey, J.E., Becker, E., Chevance, F.F.V., and Hughes, K.T. (2006) Flk prevents premature secretion of the anti-sigma factor FlgM into the periplasm. *Mol Microbiol* **60**: 630–643.

Aldridge, C., Poonchareon, K., Saini, S., Ewen, T., Soloyva, A., Rao, C.V., *et al.* (2010) The interaction dynamics of a negative feedback loop regulates flagellar number in *Salmonella enterica* serovar Typhimurium. *Mol Microbiol* **78**: 1416–1430.

Andréasson, C., Fiaux, J., Rampelt, H., Mayer, M.P., and Bukau, B. (2008) Hsp110 is a nucleotide-activated exchange factor for Hsp70. *J Biol Chem* **283**: 8877–8884.

Arricau, N., Hermant, D., Waxin, H., Ecobichon, C., Duffey, P.S., and Popoff, M.Y. (1998) The RcsB-RcsC regulatory system of *Salmonella typhi* differentially modulates the expression of invasion proteins, flagellin and Vi antigen in response to osmolarity. *Mol Microbiol* **29**: 835–850.

Baaske, P., Wienken, C.J., Reineck, P., Duhr, S., and Braun, D. (2010) Optical thermophoresis for quantifying the buffer dependence of aptamer binding. *Angew Chem Int Ed Engl* **49**: 2238–2241.

Bender, J., and Kleckner, N. (1992) IS10 transposase mutations that specifically alter target site recognition. *EMBO J* **11**: 741–750.

Bertani, G. (2004) Lysogeny at mid-twentieth century: P1, P2, and other experimental systems. *J Bacteriol* **186**: 595–600.

Castanié-Cornet, M.-P., Cam, K., Bastiat, B., Cros, A., Bordes, P., and Gutierrez, C. (2010) Acid stress response in *Escherichia coli*: mechanism of regulation of *gadA* transcription by RcsB and GadE. *Nucleic Acids Res* **38**: 3546–3554.

Chevance, F.F., and Hughes, K.T. (2008) Coordinating assembly of a bacterial macromolecular machine. *Nat Rev Microbiol* **6**: 455–465.

Chilcott, G.S., and Hughes, K.T. (2000) Coupling of flagellar gene expression to flagellar assembly in *Salmonella enterica* serovar Typhimurium and *Escherichia coli*. *Microbiol Mol Biol Rev* **64**: 694–708.

Chubiz, J.E.C., Golubeva, Y.A., Lin, D., Miller, L.D., and Slauch, J.M. (2010) FliZ regulates expression of the *Salmonella* pathogenicity island 1 invasion locus by controlling HilD protein activity in *Salmonella enterica* serovar Typhimurium. *J Bacteriol* **192**: 6261–6270.

Cordero-Alba, M., Bernal-Bayard, J., and Ramos-Morales, F. (2012) SrfJ, a *Salmonella* type III secretion system effector regulated by PhoP, RcsB, and IolR. *J Bacteriol* **194**: 4226–4236.

Delgado, M.A., Mouslim, C., and Groisman, E.A. (2006) The PmrA/PmrB and RcsC/YojN/RcsB systems control expression of the *Salmonella* O-antigen chain length determinant. *Mol Microbiol* **60**: 39–50.

Detweiler, C.S., Monack, D.M., Brodsky, I.E., Mathew, H., and Falkow, S. (2003) *virK*, *somA* and *rcsC* are important for systemic *Salmonella enterica* serovar Typhimurium infection and cationic peptide resistance. *Mol Microbiol* **48**: 385–400.

Dove, S.L., and Hochschild, A. (2004) A bacterial two-hybrid system based on transcription activation. *Methods Mol Biol* **261**: 231–246.

Duan, Q., Zhou, M., Zhu, L., and Zhu, G. (2013) Flagella and bacterial pathogenicity. *J Basic Microbiol* **53**: 1–8.

Ellermeier, C.D., and Slauch, J.M. (2003) RtsA and RtsB coordinately regulate expression of the invasion and flagellar genes in *Salmonella enterica* serovar Typhimurium. *J Bacteriol* **185**: 5096–5108.

Erhardt, M., and Hughes, K.T. (2010) C-ring requirement in flagellar type III secretion is bypassed by FlhDC upregulation. *Mol Microbiol* **75**: 376–393.

Farizano, J.V., Torres, M.A., Pescaretti, M. de L.M., and Delgado, M.A. (2014) The RcsCDB regulatory system plays a crucial role in the protection of *Salmonella enterica* serovar Typhimurium against oxidative stress. *Microbiology (Reading, Engl)* **160**: 2190–2199.

Farris, C., Sanowar, S., Bader, M.W., Pfuetzner, R., and Miller, S.I. (2010) Antimicrobial peptides activate the Rcs regulon through the outer membrane lipoprotein RcsF. *J Bacteriol* **192**: 4894–4903.

Francez-Charlot, A., Laugel, B., Van Gemert, A., Dubarry, N., Wiorowski, F., Castanié-Cornet, M.-P., *et al*. (2003) RcsCDB His-Asp phosphorelay system negatively regulates the *flhDC* operon in *Escherichia coli*. *Mol Microbiol* **49**: 823–832.

Frye, J., Karlinsey, J.E., Felise, H.R., Marzolf, B., Dowidar, N., McClelland, M., and Hughes, K.T. (2006) Identification of new flagellar genes of *Salmonella enterica* serovar Typhimurium. *J Bacteriol* **188**: 2233–2243.

García-Calderón, C.B., García-Quintanilla, M., Casadesús, J., and Ramos-Morales, F. (2005) Virulence attenuation in *Salmonella enterica rcsC* mutants with constitutive activation of the Rcs system. *Microbiology* **151**: 579–588.

García-Calderón, C.B., Casadesús, J., and Ramos-Morales, F. (2007) Rcs and PhoPQ regulatory overlap in the control of *Salmonella enterica* virulence. *J Bacteriol* **189**: 6635–6644.

Gillen, K.L., and Hughes, K.T. (1991) Molecular characterization of *flgM*, a gene encoding a negative regulator of flagellin synthesis in *Salmonella typhimurium*. *J Bacteriol* **173**: 6453–6459.

Gupte, G., Woodward, C., and Stout, V. (1997) Isolation and characterization of *rcsB* mutations that affect colanic acid capsule synthesis in *Escherichia coli* K-12. *J Bacteriol* **179**: 4328–4335.

Henikoff, S., Wallace, J.C., and Brown, J.P. (1990) Finding protein similarities with nucleotide sequence databases. *Methods Enzymol* **183**: 111–132.

Hohmann, E.L. (2001) Nontyphoidal salmonellosis. *Clin Infect Dis* **32**: 263–269.

Huang, Y.-H., Ferrières, L., and Clarke, D.J. (2006) The role of the Rcs phosphorelay in *Enterobacteriaceae*. *Res Microbiol* **157**: 206–212.

Karlinsey, J.E. (2007) λ-Red genetic engineering in *Salmonella enterica* serovar Typhimurium. In *Methods in Enzymology*. Academic Press,Volume 421, Editors Kelly T. Hughes and Stanley R. Maloy, Elsevier Inc, pp. 199–209.

Karlinsey, J.E., Tanaka, S., Bettenworth, V., Yamaguchi, S., Boos, W., Aizawa, S.I., and Hughes, K.T. (2000) Completion of the hook-basal body complex of the *Salmonella typhimurium* flagellum is coupled to FlgM secretion and *fliC* transcription. *Mol Microbiol* **37**: 1220–1231.

Kelly, A., Goldberg, M.D., Carroll, R.K., Danino, V., Hinton, J.C.D., and Dorman, C.J. (2004) A global role for Fis in the transcriptional control of metabolism and type III secretion in *Salmonella enterica* serovar Typhimurium. *Microbiology* **150**: 2037–2053.

Koirala, S., Mears, P., Sim, M., Golding, I., Chemla, Y.R., Aldridge, P.D., and Rao, C.V. (2014) A nutrient-tunable bistable switch controls motility in *Salmonella enterica* serovar Typhimurium. *MBio* **5**: e01611-14.

Kutsukake, K. (1997) Autogenous and global control of the flagellar master operon, *flhD*, in *Salmonella typhimurium*. *Mol Gen Genet* **254**: 440–448.

Latasa, C., García, B., Echeverz, M., Toledo-Arana, A., Valle, J., Campoy, S., *et al*. (2012) *Salmonella* biofilm

development depends on the phosphorylation status of RcsB. *J Bacterio* **194**: 3708–3722.
Lehnen, D., Blumer, C., Polen, T., Wackwitz, B., Wendisch, V.F., and Unden, G. (2002) LrhA as a new transcriptional key regulator of flagella, motility and chemotaxis genes in *Escherichia coli*. *Mol Microbiol* **45**: 521–532.
Lin, D., Rao, C.V., and Slauch, J.M. (2008) The *Salmonella* SPI1 type three secretion system responds to periplasmic disulfide bond status via the flagellar apparatus and the RcsCDB system. *J Bacteriol* **190**: 87–97.
Majdalani, N., and Gottesman, S. (2005) The Rcs phosphorelay: a complex signal transduction system. *Annu Rev Microbiol* **59**: 379–405.
Mariscotti, J.F., and García-del Portillo, F. (2009) Genome expression analyses revealing the modulation of the *Salmonella* Rcs regulon by the attenuator IgaA. *J Bacteriol* **191**: 1855–1867.
Mouslim, C., and Hughes, K.T. (2014) The effect of cell growth phase on the regulatory cross-talk between flagellar and Spi1 virulence gene expression. *PLoS Pathog* **10**: e1003987.
Mouslim, C., Delgado, M., and Groisman, E.A. (2004) Activation of the RcsC/YojN/RcsB phosphorelay system attenuates *Salmonella* virulence. *Mol Microbiol* **54**: 386–395.
Mouslim, C., Latifi, T., and Groisman, E.A. (2003) Signal-dependent requirement for the co-activator protein RcsA in transcription of the RcsB-regulated *ugd* gene. *J Biol Chem* **278**: 50588–50595.
Pfaffl, M.W. (2001) A new mathematical model for relative quantification in real-time RT-PCR. *Nucleic Acids Res* **29**: 2002–2007.
Salscheider, S.L., Jahn, A., and Schnetz, K. (2014) Transcriptional regulation by BglJ-RcsB, a pleiotropic heteromeric activator in *Escherichia coli*. *Nucleic Acids Res* **42**: 2999–3008.
Sanderson, K.E., and Roth, J.R. (1988) Linkage map of *Salmonella typhimurium*, edition VII. *Microbiol Rev* **52**: 485–532.
Sato, Y., Takaya, A., Mouslim, C., Hughes, K.T., and Yamamoto, T. (2014) FliT selectively enhances proteolysis of FlhC subunit in $FlhD_4C_2$ complex by an ATP-dependent protease, ClpXP. *J Biol Chem* **289**: 33001–33011.
Singer, H.M., Erhardt, M., and Hughes, K.T. (2013) RflM functions as a transcriptional repressor on the autogenous control of the *Salmonella* flagellar master operon *flhDC*. *J Bacteriol* **195**: 4274–5382.
Singer, H.M., Kühne, C., Deditius, J.A., Hughes, K.T., and Erhardt, M. (2014) The *Salmonella* Spi1 virulence regulatory protein HilD directly activates transcription of the flagellar master operon *flhDC*. *J Bacteriol* **196**: 1448–1457.
Sledjeski, D.D., and Gottesman, S. (1996) Osmotic shock induction of capsule synthesis in *Escherichia coli* K-12. *J Bacteriol* **178**: 1204–1206.
Stout, V., Torres-Cabassa, A., Maurizi, M.R., Gutnick, D., and Gottesman, S. (1991) RcsA, an unstable positive regulator of capsular polysaccharide synthesis. *J Bacteriol* **173**: 1738–1747.
Takaya, A., Erhardt, M., Karata, K., Winterberg, K., Yamamoto, T., and Hughes, K.T. (2012) YdiV: a dual function protein that targets FlhDC for ClpXP-dependent degradation by promoting release of DNA-bound FlhDC complex. *Mol Microbiol* **83**: 1268–1284.
Tarazona, M.S., and Saiz, E. (2003) Combination of SEC/MALS experimental procedures and theoretical analysis for studying the solution properties of macromolecules. *J Biochem Biophys Methods* **56**: 95–116.
Uzzau, S., Figueroa-Bossi, N., Rubino, S., and Bossi, L. (2001) Epitope tagging of chromosomal genes in *Salmonella*. *Proc Natl Acad Sci USA* **98**: 15264–15269.
Venkatesh, G.R., Kembou Koungni, F.C., Paukner, A., Stratmann, T., Blissenbach, B., and Schnetz, K. (2010) BglJ-RcsB heterodimers relieve repression of the *Escherichia coli bgl* operon by H-NS. *J Bacteriol* **192**: 6456–6464.
Virlogeux, I., Waxin, H., Ecobichon, C., Lee, J.O., and Popoff, M.Y. (1996) Characterization of the *rcsA* and *rcsB* genes from *Salmonella typhi*: *rcsB* through *tviA* is involved in regulation of Vi antigen synthesis. *J Bacteriol* **178**: 1691–1698.
Wada, T., Tanabe, Y., and Kutsukake, K. (2011) FliZ acts as a repressor of the *ydiV* gene, which encodes an anti-$FlhD_4C_2$ factor of the flagellar regulon in *Salmonella enterica* serovar Typhimurium. *J Bacteriol* **193**: 5191–5198.
Wang, Q., and Harshey, R.M. (2009) Rcs signalling-activated transcription of *rcsA* induces strong anti-sense transcription of upstream *fliPQR* flagellar genes from a weak intergenic promoter: regulatory roles for the anti-sense transcript in virulence and motility. *Mol Microbiol* **74**: 71–84.
Wang, Q., Zhao, Y., McClelland, M., and Harshey, R.M. (2007) The RcsCDB signaling system and swarming motility in *Salmonella enterica* serovar Typhimurium: dual regulation of flagellar and SPI-2 virulence genes. *J Bacteriol* **189**: 8447–8457.
Wehland, M., and Bernhard, F. (2000) The RcsAB box. Characterization of a new operator essential for the regulation of exopolysaccharide biosynthesis in enteric bacteria. *J Biol Chem* **275**: 7013–7020.
Wozniak, C.E., Lee, C., and Hughes, K.T. (2009) T-POP array identifies EcnR and PefI-SrgD as novel regulators of flagellar gene expression. *J Bacteriol* **191**: 1498–508.
Wyatt, P.J. (1993) Light scattering and the absolute characterization of macromolecules. *Anal Chim Acta* **272**: 1–40.
Yamamoto, S., and Kutsukake, K. (2006) FliT acts as an anti-$FlhD_2C_2$ factor in the transcriptional control of the flagellar regulon in *Salmonella enterica* serovar Typhimurium. *J Bacteriol* **188**: 6703–6708.
Yanagihara, S., Iyoda, S., Ohnishi, K., Iiono, T., and Kutsukake, K. (1999) Structure and transcriptional control of the flagellar master operon of *Salmonella typhimurium*. *Genes Gen Syst* **74**: 105–111.

Supporting information

Additional supporting information may be found in the online version